

Scheduling and Power Control for Wireless Multicast Systems via Deep Reinforcement Learning[†]

Ramkumar Raghu¹, Mahadesh Panju¹, Vaneet Aggarwal^{1,2}, and Vinod Sharma¹

¹Indian Institute of Science, Bangalore, INDIA. {ramkumar,mahadesh,vinod}@iisc.ac.in

²Purdue University, West Lafayette IN, USA. vaneet@purdue.edu

Abstract—Multicasting in wireless systems is a natural way to exploit the redundancy in user requests in a Content Centric Network. Power control and optimal scheduling can significantly improve the wireless multicast networks performance under fading. However, the model-based approaches for power control and scheduling studied earlier are not scalable to large state space or changing system dynamics. In this paper, we use deep reinforcement learning where we use function approximation of the Q-function via a deep neural network to obtain a power control policy that matches the optimal policy for a small network. We show that power control policy can be learnt for reasonably large systems via this approach. Further we use multi-timescale stochastic optimization to maintain the average power constraint. We demonstrate that a slight modification of the learning algorithm allows tracking of time varying system statistics. Finally, we extend the multi-time scale approach to simultaneously learn the optimal queueing strategy along with power control. We demonstrate scalability, tracking and cross-layer optimization capabilities of our algorithms via simulations. The proposed multi-time scale approach can be used in general large state-space dynamical systems with multiple objectives and constraints, and may be of independent interest.

Index Terms—Multicasting, Scheduling, Queueing, Deep Reinforcement Learning, Quality of Service, Power Control, Dynamics Tracking, Multi-timescale Stochastic Optimization.

I. INTRODUCTION

Content services such as Netflix, Prime Video, etc., have dramatically increased the demand for high-definition videos over mobile networks. Almost 78% of mobile data traffic is expected to be due to these mobile videos [1]. It is observed that the request traffic for these contents have multiple redundant requests [2]. Next generation wireless networks are being constantly upgraded to satisfy these exploding demands by exploiting the nature of the request traffic. Serving the redundant requests simultaneously is a natural way to utilize network resources efficiently. Thus, efficient multicasting is studied widely in the wireless networking community.

A multicast queue with network coding is studied in [3] with an infinite library of files. The case of slotted broadcast systems with one server transmitting to multiple users is studied in [4]. Some recent works [5] use coded caching to achieve multicast. This approach uses local information in the user caches to decode the coded transmission and provides improvement in throughput by increasing the effective number

of files transferred per transmission. This throughput may get reduced in a practical scenario due to queueing delays at the basestation/server. [6] addresses these issues, analyses the queueing delays and compares it with an alternate coded scheme with LRU caches (CDLS) which provides improvement over the coded schemes in [5]. A more recent work in this direction, [7] provides alternate multicast schemes and analyses queueing delays for such multicast systems. In [7], it is shown that a simple multicast scheme, can have significant gains over the schemes in [5], [6] in high traffic regime.

We further study the multicast scheme proposed in [7] in this paper. This multicast queue merges the requests for a given file from different users, arriving during the waiting time of the initial requests. The merged requests are then served simultaneously. The gains achieved by this simple multicast scheme, however, are quickly lost in wireless channels due to fading. It suffers from the users with bad channels, thereby decreasing the QoS even for users with good channels. The authors of [8] studied this problem and proposed novel schemes, which provide significant multicast gains under fading as compared to the simple multicast. Further, it was shown that an optimal state dependent power control can significantly improve the average delays experienced by the users.

The queueing schemes and the power control policy proposed in [8], though provide improved delays, have following limitations. 1) The queueing scheme which performs best depends on the system parameters such as size of the system, the request rate, etc. 2) The algorithm to obtain the power control policy is not scalable with the number of users and the number of states of the channel gains. Also, the policy doesn't adapt to changing system statistics, which in turn depends on the power control policy. 3) The queueing schemes and power control are dealt individually. This paper tries to overcome the above limitations of the scheme in [8].

We first provide algorithms for the two optimization problems individually and then combine the two algorithms to obtain the overall optimal queueing strategy and the power control. Stochastic optimization ([9]) is a useful tool to obtain the optimally parametrized queueing strategy. However, for convergence of stochastic optimization algorithms, a careful approximation of stochastic gradients is necessary. One challenge here is that the cost to be optimized is the mean stationary sojourn time of requests to be delivered. We propose a new Deep Assisted Gradient Approximation algorithm, where, the

[†]Preliminary version of a part of this paper was presented in Allerton, 2019.

novelty is in deriving the gradients from a Deep Network assisted by a memory. This memory helps retain the history of the explored regions and also allows adaptation to changing system dynamics in an online fashion. The replay memory and online training of the deep network adds an important feature called Importance Sampling to the stochastic optimization, which improves the confidence (lower variance) in the gradient descent steps.

Multicast systems with power control can be conveniently modeled as Markov Decision Process (MDP) but with large state and action spaces. Obtaining transition probabilities and the optimal policy, however, for such large MDPs is not feasible. Reinforcement learning, particularly, Deep reinforcement learning [10], comes as a natural tool to address such problems. Reinforcement learning can be used even when the transition probabilities are not available. However, large state/action space can still be an issue. Using function approximation via deep neural networks can provide significant gains. Several deep reinforcement learning techniques such as Deep Q-Network [11], Trust Region Policy Optimization (TRPO) [12], Proximal Policy Gradient (PPO) [13], etc. have been successfully applied to several large state-space dynamical systems such as Atari [14], AlphaGo [15], etc. DQN is based on value iteration. TRPO and PPO are policy gradient based methods. Policy-Gradient methods often suffer from high variance in sample estimates and poor sample efficiency [10]. Value iteration based deep RL methods, like DQN, have been theoretically shown to have better performance [16] due to target network and Replay memory and provide global minimum.

We propose a constrained optimization variant of DQN based on multi-timescale stochastic gradient descent [9] for power control which can track the system statistics. Finally, we develop an algorithm which combines the above two algorithms to obtain an optimal queuing strategy and power control policy.

The major contributions of this paper are as follows:

- A novel deep assisted stochastic gradient descent (DSGD) algorithm for obtaining the best queuing strategy from a given set.
- Proposing two modifications to DQN to accommodate constraints and system adaptations. The constraints can be met by using a Lagrange multiplier. The appropriate Lagrange multiplier is also learnt via a two time scale stochastic gradient descent. We call this algorithm Adaptive Constrained DQN (AC-DQN).
- Unlike DQN, AC-DQN can be applied to the multicast systems with constraints, as in [8], to learn the power control policy, online. The proposed method meets the average power constraint while achieving the global optima as achieved by the static policy proposed in [8] for a small scale setup of the problem.
- We demonstrate the scalability of our algorithms with system size (number of users, arrival rate, complex fading).
- We show that AC-DQN can track the changes in the dynamics of the system, e.g., change of rate of arrival over the time of a day, and achieve optimal performance.

- Finally, using the above two algorithms, we propose a generalized algorithm called Integrated DSGD and AC-DQN (IDA) to optimize systems with multiple objectives and constraints. Particularly, this algorithm is useful in any wireless network with cross-layer objectives, such as ours. IDA is a three time scale stochastic optimization algorithm for obtaining both the queuing strategy (unconstrained network layer objective) and power control (constrained physical layer objective), simultaneously.

We show via simulations that our algorithms choose the optimal policy among the given set of policies. Also, the power control policy obtained via our algorithm improves the delay performance of the multicast network by more than 50% compared to the constant power policy. Our algorithms work equally well when we replace DQN with its improvements such as DDQN [17]. In fact we have run our simulations with DDQN variant of AC-DQN and have achieved similar performance.

A. Related Works

Queueing and Power control in Multicast Systems: Multicast Queue and Scheduling has been studied in [3], [18]–[20]. The works in [3], [18], [19] propose schemes for network coded multicast systems and analyse stability of the proposed multicast queues. Unlike these works, we use, as in our previous work [7], [8], a simple uncoded multicast queue which is always stable. In [7], we show that our queueing schemes perform much better than the coded multicast schemes in high traffic regimes. In the current work, we improve over the results in [7] and [8] by providing novel deep learning based queueing strategies. [20] proposes a multicast scheduling scheme for Poisson traffic. However, there's no power control and the proposed queue is not always stable.

Power control in multicast systems has been studied in [21], [22]. In [21], power allocation optimizes the ergodic capacity while maintaining certain minimum rate requirements at the users and average power constraints. In [22], the authors minimize a utility function via linear programming, under SINR constraints at the users and transmit power constraints at the transmitter. Both [21], [22] derive an optimal power control policy for delivery to all the users, whereas this paper considers delivery to a random subset of users requesting file at that time. Also, the power control policies in [21], [22], require knowledge of system statistics and are not scalable for our system. Our scheme is computationally scalable, does not require knowledge of system statistics (traffic intensity, fading distributions) and can track changing system statistics.

Deep Learning in Wireless Multicast systems: The ability of DeepRL to handle large state-space dynamic systems is being exploited in various multicast wireless systems/networks. In [23], the authors study a resource allocation problem in unicast and broadcast transmissions. The DeepRL agent learns and selects power and frequency for each channel to improve rate under some latency constraints. Like in our work, they also introduce constraints via Lagrange multipliers. However, the Lagrange multiplier is constant and the agent does not

learn it. Thus, the agent also does not adapt if the system dynamics changes as the Lagrange constant is fixed and the learning rate decays with time. To get the appropriate Lagrange multiplier is computationally expensive and requires known system statistics. Another work, [24], applies unconstrained deep reinforcement learning to multiple transmitters for a proportionally fair scheduling policy by adjusting individual transmit powers. [25] applies DeepRL in queueing in a coded caching based multicast system which is shown to be inferior to our multicast schemes in high traffic rate region. For more literature on Deep Learning applications to wireless multicast systems, see the detailed survey [26].

For Constrained MDPs see [27]. However these algorithms are not scalable. [28] introduced constrained reinforcement learning algorithm based on Trust Region Policy optimization. Unlike our case this approach uses discounted constraints. Also, this algorithm requires multiple evaluations of policies and sample paths to reduce the estimator variance. Though this algorithm may perform very well on simulated systems like Atari [14], AlphaGo [15], etc., it is not suitable for practical systems where, more often than not, we cannot have multiple evaluations of different policies and sample paths. In [29], a Lagrange based actor critic approach for constrained RL, is proposed. Since this is also a policy based approach this also suffers from high variance when multiple evaluations are infeasible. In [30], an alternate approach with two value functions for reward and constraint (cost) with actor-critic policy update, is proposed. Here, at each step a convex relaxation based optimization is used to get the optimal parameter of value functions. We note that the convex optimization step at each iterate is computationally more intensive than a simple SGD step. Thus the above mentioned policy iteration methods either have high variance in practical systems or are computationally intensive. These issues make it difficult to track the changing dynamics in practical systems, as we can in our case. To the best of our knowledge ours is the first constrained value iteration based Deep RL algorithm for constrained MDPs. The use of replay memory and a target network helps reduce estimator variance in our algorithm. These features also increase the practical applicability of our algorithm.

Rest of the paper is organised as follows. Section II explains the system model and motivates the problem. Section III presents our deep learning based optimal queueing algorithm. Section IV motivates the power control problem and briefly explains the power control algorithm proposed in [8]. Section V presents the proposed DeepRL algorithm AC-DQN for scalable, improved power control. Section VI presents our novel deep multi-timescale algorithm to achieve scalable cross-layer optimization of queueing and power control and provides optimal performance for the multicast system. Section VII demonstrates our algorithms via simulations and Section VIII concludes the paper.

II. SYSTEM MODEL

We consider a system with one server transmitting files from a fixed finite library to a set of users (Figure 1). We denote

the set of users by $\mathcal{L} = \{1, 2, \dots, L\}$ and the set of files by $\mathcal{M} = \{1, 2, \dots, M\}$. The request process for file i from user j is a Poisson process of rate λ_{ij} which is independent of the request processes of other files from user j and also from other users. The total arrival rate is $\lambda = \sum_{i,j} \lambda_{ij}$. The requests of a file from each user are queued at the server till the user successfully receives the file. All the files are of length F bits. The server transmits at a fixed rate, R bits/sec. Thus, the transmission time for each file is $T = F/R$.

The channels between the server and the users experience time varying fading. The channel gain of each user is assumed to be constant during transmission of a file. The channel gain for the j^{th} user at the t^{th} transmission, is represented by $H_j(t)$. Each $H_j(t)$ takes values in a finite set and form an independent identically distributed (i.i.d) sequence in time, as in [31]. The channel gains of different users are independent of each other and may have different distributions. Let $H = (H_1, \dots, H_L)$.

Since the requests from the users are queued at the server, every request awaits its turn for transmission and thus experiences a queueing delay which is random in nature. The distribution of this random delay depends on the queueing policy. Also, unsuccessful transmissions due to fading, adds further delay, experienced by each request. We denote by random variable D , the overall delay experienced by each request due to both queueing and fading. If t_A is the time of arrival of a request to the server and t_S is time instance representing the end of successful transmission/service of the request. Then the random delay/sojourn time D is given by $D = t_S - t_A$. Further, $E[D]$ denotes the stationary mean sojourn time experienced by each request.

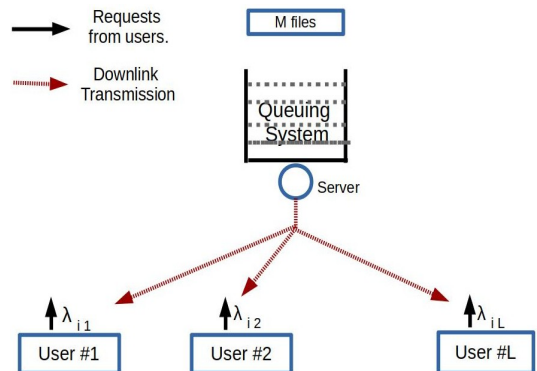


Fig. 1: System model

More details of the system are described in the following sections as follows. Section II-A describes the basic Multicast queue proposed in [7]. The queueing schemes to mitigate the effects of fading studied in [8] are also presented. Section II-B parametrizes the queueing schemes. Section III provides an online learning scheme to obtain the optimal policy for a given setup. In Sections IV-A and IV-B, we summarise the results from [8], which show that using power control can further improve the performance and the algorithm used to obtain the optimal power policy. We will see that this algorithm is not scalable. Then in Section IV-C we provide the MDP of the power control problem. In Section V we will present the

scalable DeepRL solution for this formulation.

A. Multicast Queue

For scheduling transmissions at the server, we consider the *multicast queue* studied in [8]. In this system, the requests for different files from different users are queued in a single queue, called the multicast queue. In this queue, the requests for file i from all users are merged and considered as a single request. The requested file and the users requesting it, is denoted by (i, \mathbb{L}_i) . In other words, \mathbb{L}_i is the list of users interested in file i . A new request for file i , from user j is merged with the corresponding entry \mathbb{L}_i , if it already exists. Else, it is appended to the tail of the queue. Service/transmission of file i , serves all the users in \mathbb{L}_i , possibly with errors due to channel fading.

The random subset of users served by the multicast queue at the t^{th} transmission, is denoted by the random binary vector, $V(t) = (V_1(t), \dots, V_L(t))$, where $V_j(t) = 1$ implies that the user j has requested the file being transmitted; otherwise, $V_j(t) = 0$. From [Theorem 1, [7]], $V(t)$ has a unique stationary distribution.

It was shown in [7] that the above multicast queue performs much better than the multicast queues proposed in literature before. *The main difference compared to previous multicast schemes is that in this scheme, all requests of all the users for a given file are merged together over time. One direct consequence of this is that the queue length at the base station does not exceed M . Thus the delay is bounded for all traffic rates. In fact the mean delays are often better than the coded caching schemes proposed in the literature, as well, for most of the traffic conditions.*

In a fading scenario, where the different users have independent fading, the performance of this scheme can significantly deteriorate because of multiple retransmissions required to successfully transmit to all the users needed. Thus, in [8], multiple queuing strategies were proposed and compared to recover the performance of the system and reduce the mean delay substantially. Some of these are also fair to different users in the sense, that the users with good channel gains do not suffer due to users with bad channel gains. We now briefly present the schemes proposed in [7], [8] for clarity.

Retransmit: This is the simplest scheme proposed in [7]. Here the multicast queue is serviced from head to tail. The head of the line is retransmitted until all the users in it are serviced. The new requests are added to the queue in a similar manner to the simple multicast. This naive scheme works very well in low request rate regime, however performs poorly in the high request rates and severely deteriorates delays experienced by users with good channels.

Single queue with loop-back (1-LB): The Multicast queue is serviced from head to tail. When a file is transmitted, some of the users will receive the file successfully and some users may receive the file with errors. In the case of unsuccessful reception by some users, the file is retransmitted. A maximum of N ($1 \leq N \leq \infty$) transmission attempts are made. If there are some users who did not receive the file within N transmission attempts, the request (tuple (i, \mathbb{L}_i) with \mathbb{L}_i , now modified to contain only the set of users who have not received the file

i successfully) is fed back to the queue. If there is another pending request in the queue for the same file (a request for the file which came during the current transmission), it is merged with the existing request. Otherwise, a new request for the same file with unsuccessful users is inserted at the tail of the queue.

Defer Queue with loop back (2-LB): This strategy has two queues for servicing the requests. A multicast queue and a defer queue. The multicast queue is similar to the queue mentioned in the beginning of this section and is serviced from head to tail. The defer queue is an additional queue to handle unsuccessful transmissions as follows. When a file is transmitted, some users may receive the file with errors. In the case of unsuccessful reception by some users after a maximum of N transmissions, the file request and the unserved users are queued in the defer queue. Such requests stay in the defer queue until a new request for the same file arrives. On the arrival of the new request, the new request is merged with the older requests in the defer queue and moved to the tail of the multicast queue. If no such old requests exist in the defer queue, the new request is merged/added to the multicast queue. This queue is shown to provide lower delay to good channel users than to bad channel users.

Performance of each of these queues, depends on system parameters, transmission power policy, arrival rate, etc. For simplicity of presentation we consider the case of $N = 1$ for all the queueing strategies, in this paper.

B. Parametrization of Queueing Strategies

To adaptively optimize the queueing strategy according to system parameters, it is convenient to first parametrize them. We propose a simple parametrization using probabilities for each queueing strategy. That is, at the end of every service instance if some users did not get the file successfully, the multicast queue chooses to retransmit the head of the line (HoL) request with probability p_1 , loopback HoL with probability p_2 or defer HoL with probability p_3 , such that $\sum_{j=1}^3 p_j = 1$. Thus, $\bar{p} = [p_1, p_2, p_3]$ parametrizes the queueing strategy. Here, $\bar{p} \in \mathbb{P}$, where \mathbb{P} is the probability simplex, $\mathbb{P} = \{[p_1, p_2, p_3] \in [0, 1]^3 : \sum_{j=1}^3 p_j = 1\}$. Observe, that $\bar{p} = [1, 0, 0]$, $[0, 1, 0]$, and $[0, 0, 1]$ represent retransmit, loopback, and defer strategies. In the next section we provide an algorithm to get optimal \bar{p} .

III. DEEP LEARNING FOR OPTIMAL QUEUEING

We are interested in finding the optimal \bar{p} among the parametrized queueing strategies in Section II-B that gives the least average delay. From our previous work (Proposition 1, [7]), it can be shown that for any parameter \bar{p} there exists a stationary mean sojourn time, $E_{\bar{p}}[D]$, where D is the sojourn time and E is the expectation. In this section we propose an online deep learning algorithm to learn $\bar{p}^* = \underset{\bar{p} \in \mathbb{P}}{\operatorname{argmin}} E_{\bar{p}}[D]$.

However, the map $f : \bar{p} \mapsto E_{\bar{p}}[D]$ is quite complex and it is very difficult to obtain its closed form expression.

Since we do not have a closed form expression, we depend on noisy observations of f , the mean sojourn time, from

the system to get the optimal strategy, \bar{p}^* . Here is where Deep Neural Network (DNN) fits in. They are state-of-the-art tools used for several learning problems, especially regression. Before we proceed with motivation for using DNN, it is worth mentioning that several stochastic approximation algorithms, such as simultaneous perturbation stochastic approximation ([32], pg 41-76), exist for such noisy function optimization. However, convergence of such algorithms are prone to high variance in the gradient estimate and often lead to suboptimal results. In fact we have tried SF-SPSA ([32], pg 77-102), in our system and have seen that the algorithm leads to a suboptimal point in many cases. ReLU (Rectified Linear Unit) based Deep Neural Networks (DNN) on the other hand are adept at approximating such complex functions on compact subsets such as \mathbb{P} , [33]. Particularly, it is seen that DNN can provide better generalization in function approximation even with noisy training data [34]. Further, DNNs are also known to provide good gradient approximates for the approximated function, [35]. This motivates us to use DNN to approximate $f(\bar{p})$ as $f_\theta(\bar{p})$, where θ is the weight parameter of the DNN. Further the gradients required for optimization are derived using finite difference method on $f_\theta(\bar{p})$. Another important feature of our algorithm is the Replay Memory. This idea is borrowed from the Reinforcement Learning setting [36]. It helps us in storing previously seen noisy function observations and use it for training the DNN in online fashion.

The replay memory and online training of the DNN are the important features of our algorithm. Online training inherently adds Importance Sampling [37] feature to our algorithm, that is, we train our neural network only with samples that are more informative. This is shown to accelerate DNN training time [37]. We will see in our algorithm that this happens naturally as training samples for the neural network come from the parameter \bar{p} update step. These samples give more information about the neighbourhood of the point the algorithm is currently in, thereby improving the confidence/variance in the descent direction. We now present our algorithm, Deep assisted Stochastic Gradient Descent for obtaining the optimal queueing strategy.

A. Deep assisted Stochastic Gradient Descent (DSGD)

Our algorithm, has three steps:

- Generating Noisy observation \hat{f} of the function f at random points and storing in replay memory, \mathbb{M}_D . This provides us the initial training set.

To obtain \hat{f} for a randomly generated point \bar{p} , the system is set to follow policy \bar{p} and run till S_{approx} services are completed. Let, d_i be the sojourn time of i^{th} successfully served request in S_{approx} services. These are stored in a temporary memory \bar{D} . From $d_i, i \in [|\bar{D}|]$ compute:

$$\hat{f} = \frac{1}{|\bar{D}|} \sum_{i=1}^{|\bar{D}|} d_i \quad (1)$$

The point (\bar{p}, \hat{f}) is stored in \mathbb{M}_D and \bar{D} is cleared.

- Sample a minibatch of points from \mathbb{M}_D , uniformly randomly and train f_θ :

$$\theta \leftarrow \theta - \eta_1 \nabla_\theta L_{f_\theta} \quad (2)$$

where, L_{f_θ} is the Mean Square Error obtained from minibatch sampled from the replay memory, given by $L_{f_\theta} = \sum_{i=1}^n (f_\theta(\bar{p}_i) - \hat{f}_i)^2 / n$.

- Obtain numerical gradient of f_θ at the last executed point \bar{p} and perform a gradient descent:

$$\bar{p} \leftarrow \mathcal{P}(\bar{p} - \eta_2 \nabla_{\bar{p}} f_\theta(\bar{p})) \quad (3)$$

Get the noisy observation of f at the new point. Store the new (\bar{p}, \hat{f}) to the replay memory, \mathbb{M}_D . \mathcal{P} is the projection operator that projects the input to the probability simplex as,

$$\mathcal{P}[r_1, r_2, r_3] = \{[r_1, r_2, r_3]\}^+ / \sum_{i=1}^3 \{r_i\}^+ \quad (4)$$

where element wise operator $\{\cdot\}^+ = \max\{0, \cdot\}$, and $r_i \in \mathbb{R}$, $i = 1, 2, 3$.

- η_1 and η_2 are learning parameters and must follow learning rate relationships of multi-timescale stochastic gradient descent, [9], given in (17) in Section V. The detailed algorithm is given in Algorithm 1.

Algorithm 1: Deep assisted Stochastic Gradient Descent (DSGD) Algorithm

Input:

Multicast system in II-A, Replay Memory: \mathbb{M}_D ,

Minibatch size: n , Training Time: T_{train} ,

Approximation Window: S_{approx} , Initialize neural

network weights: θ of f_θ , Exploration Parameter:

$\epsilon(t) \rightarrow 0$, θ , \bar{p} learning rates: $\eta_1(t)$, $\eta_2(t)$ must satisfy

(17), Simulation Time: T , Algorithm timeline: t ,

Multicast System timeline: s

for $t = 1$ to T do

if $(t < T_{train})$ then

$\bar{p} \leftarrow \mathcal{P}(Unif([0, 1]^3))$

else

Sample: Minibatch n from \mathbb{M}_D

 /*Perform DNN θ update and \bar{p} parameter update as follows:*/

$\theta \leftarrow \theta - \eta_1 \nabla_\theta L_{f_\theta}$

$\bar{p} \leftarrow \mathcal{P}(\bar{p} - \eta_2 \nabla_{\bar{p}} f_\theta + Unif([0, \epsilon_t]^3))$

end

run S_{approx} Multicast services with strategy \bar{p} and

store d_i 's in \bar{D}

obtain \hat{f} , as in (1) \rightarrow clear \bar{D}

store (\bar{p}, \hat{f}) in \mathbb{M}_D

end

$\bar{p}^* \leftarrow \bar{p}$

Output: \bar{p}^* : Optimal Queueing Strategy

We note the following:

- Initial training phase is necessary to avoid pathological zero gradients in the initial steps, which may inhibit further exploration of the function.
- The noise exploration in the second SGD step is also for the same reason.
- Minibatch sampling with Replay memory is to provide IID data samples to the DNN training, which is necessary for better generalization.

- It is natural to observe that a larger initial training phase and an offline training of DNN may avoid Replay memory during the second SGD learning phase. It is not advisable for the following reasons:

1) At any given point, \bar{p} , it is important to have a good estimate (low variance) of the descent direction in (3). For this it is essential that the DNN approximates the function well in the neighbourhood of \bar{p} . In online training this comes naturally, as the consecutive SGD steps in (3) add more points from this neighbourhood in the replay memory. This is true even if the variance in the gradient estimates are high as the steps in (3) do not go too far, when the learning rate is chosen appropriately. As the algorithm progresses, more points in neighbourhood are added and the variance in the gradient estimates naturally reduces. This is how our algorithm increases confidence in descent direction using Importance Sampling. To achieve this confidence, with offline training of DNN, it would require prohibitively large training sample set, obtained using Monte Carlo evaluations of f .

2) Further with offline training of DNN, the algorithm will not be adaptive if the system dynamics like rates, popularity etc., change. We will see that online training using replay memory is particularly useful when we integrate this algorithm with our power control algorithm.

- The SGD steps can be replaced with the improvements such as AdamOptimizer [38] for annealing of the gradients, which helps in stable gradient descent. Infact, we use Adam optimizer in all our SGD steps.

Section VII-B provides the simulation results of DSGD for a multicast system with constant transmit power.

IV. POWER CONTROL FOR MULTICAST QUEUE

We now proceed to describe the power control in the Multicast setup. Adapting the transmit power based on system and environment state under certain system constraints helps in providing the power control that may improve QoS, which is quantified by mean user delay under stationarity. It was shown in [8] that choosing the transmit power based on the channel gains, the system performance improves. We describe the system constraint, a power control model and the MADS Power control algorithm proposed in [8] in this section. We then end this section with the Markov Decision Process Formulation of the entire system that aids in development of the Deep Reinforcement Learning Based Power Control algorithm.

A. Average Power Constraint

Depending on the value of $H(t)$ and $V(t)$ at time t , the server chooses transmit power P_t , based on a power control policy $P_t = \pi(H(t), V(t))$. Choosing a good power control policy is the topic of this section. The state, S_t of the system at time t is $(H(t), V(t))$. Let P_{S_t} be the power chosen by a policy for state S_t and $R(S_t, P_{S_t})$ be the number of successful transmissions for the selected power P_{S_t} , during the t^{th} service.

For a fixed transmission rate C and for a given channel gain $H(t)$ of users, the transmit power requirement P_{req} (from Shannon's Formula) for user j is (assuming file length is long enough)

$$P_{req}(j, S_t) = \frac{N_g}{H_j^2(t)} (2^{C/B} - 1), \quad (5)$$

where, B is the bandwidth and N_g is the Gaussian noise power at receiver j . Here, for simplicity, we are taking the ideal Shannon formula in (5), which can be easily modified to make it more realistic ([39], Chapter 14). Thus the reward for the chosen power control policy, during t^{th} transmission is given by,

$$R(S_t, P_{S_t}) = \sum_{j=1}^L V_{j, S_t} 1_{\{P_{S_t} > P_{req}(j, S_t)\}}(t), \quad (6)$$

where $V_{j, S_t} = 1$ if the user j has requested the file in service and $V_{j, S_t} = 0$ otherwise. We now describe the Mesh Adaptive Direct Search (MADS) power control policy.

B. MADS Power control policy

The power control policy in [8] is derived from the following optimization problem,

$$\begin{aligned} & \max_{\{P_1, \dots, P_K\}} \sum_{k=1}^K q_k R_k \\ \text{s.t. } & \sum_{k=1}^K q_k P_k \leq \bar{P} \text{ and } P_k \geq 0, k = 1, \dots, K, \end{aligned} \quad (7)$$

where \bar{P} is the average power constraint, K is the total number of states, P_k is the power chosen by the policy in state k , q_k is the stationary distribution of state $k \in \{1, \dots, K\}$ and are assumed to be known apriori, and R_k is the reward for state k , given as $R_k = R(S_t = k, P_t = P_k)$. This is a non-convex optimization problem since the reward in Eq. (6) is a simple function (linear combination of indicators). Mesh Adaptive Direct Search (MADS) [40] is used in [8] to solve this constrained optimization problem and obtain the power control policy. Though MADS achieves global optimum, it is not scalable as its computational complexity is very high.

The state space and action space of this problem can be very high even for a moderate number of users and channel gains, e.g., a system with L users and G channel gain states, has $\mathcal{O}(2^L G^L)$ states. Therefore, in this paper we propose a deep reinforcement learning framework. This not only provides optimal solution for a reasonably large system but does so without knowing the arrival rates and channel gain statistics. In addition, we show via simulations that we can track an optimal solution even when the arrival and channel gain statistics change with time.

C. MDP Formulation

The above system can be formulated into a finite state, action Markov Decision Process denoted by tuple $(\mathbb{S}, \mathbb{A}, r, \mathbf{P}, \gamma)$: (state space, action space, reward, transition probability, discount factor), where, transition probability $\mathbf{P}(S_{t+1}|S_0, P_0, \dots, S_t, P_t) = \mathbf{P}(S_{t+1}|S_t, P_t)$, policy π chooses

power $P_t \sim \pi(\cdot|S_t)$ in state S_t and the instantaneous reward $r_t = R(S_t, P_t)$.

The action-value function [41] for this discounted MDP for policy π is

$$Q^\pi(s, a) = \mathbb{E}\left[\sum_{t=0}^{\infty} \gamma^t r_t | S_0 = s, P_0 = a\right]. \quad (8)$$

where $0 < \gamma < 1$. The optimal Q -function, Q^* is given by $Q^*(s, a) = \max_{\pi} Q^\pi(s, a)$ and satisfies the optimality relation,

$$Q^*(s, a) = r(s, a) + \max_{a'} \gamma \mathbb{E}[Q^*(s', a')], \quad (9)$$

where, s' is sampled with distribution $\mathbf{P}(\cdot|s, a)$. If we know the optimal Q -function (Q^*), we can compute the optimal policy via $\pi(s) = \arg \max_{a'} Q^*(s, a)$. We know the transition matrix of this system and hence can compute the Q -function. But the state space is very large even for a small number of users, rendering the computations infeasible. Thus, we use a parametric function approximation of the Q function via Deep neural networks and use DeepRL algorithms to get the optimal Q^* . Our cost function is stationary mean sojourn time. To get a policy which minimizes this, we actually should be working with average cost MDP instead of discounted MDP. However, the RL formulation for this problem has been defined for the discounted case, the average case being more complicated. But if we take the discount factor gamma close enough to 1, then the optimal policy obtained via the discounted problem is often close to the average case problem.

Further, to introduce the average power constraint in the MDP formulation, we look at the policies achieving

$$Q^*(s, a) = \max_{\pi: C_P \leq \bar{P}} Q^\pi(s, a) \quad (10)$$

where

$$C_P = \mathbb{E}\left[\lim_{T \rightarrow \infty} \frac{\sum_{t=0}^T P_t}{T}\right] \quad (11)$$

is the long term average power. We use the Lagrange method for constrained MDPs [27] to achieve the optimal policy. In this method, the instantaneous reward is modified as

$$r_t = R(S_t, P_t) - \beta P_t, \quad (12)$$

where, β is the Lagrange constant achieving optimal Q^* while maintaining, $C_P \leq \bar{P}$. Choosing β wrongly will provide the optimal policy with average power constraint different from \bar{P} .

V. DEEP REINFORCEMENT LEARNING BASED POWER CONTROL POLICY

In this section, we describe Deep-Q-Network (DQN) [11] based power control. First we describe the DQN algorithm. We then propose a variant of DQN for constrained problems, where in, we use a Lagrange multiplier to take care of the average power constraint. We use multi-time scale stochastic gradient descent approach to also learn the Lagrange multiplier, to obtain the right average power constraint. Finally, we change the learning step size from decreasing to a constant so that the optimal power control can track the time varying system statistics.

A. Deep Q Networks

DQN is a popular Deep Reinforcement learning algorithm to handle large state-space MDPs with unknown/complex dynamics, $\mathbf{P}(S_{t+1}|S_t, P_t)$. The DQN is a Value Iteration based method, where the action-value function is approximated by a Neural Network. Though there are several follow up works providing improvements over this algorithm [17], [42], we use this algorithm owing to its simplicity. We will show that DQN itself is able to provide us the optimal solution and tracking. These improvements may further improve the performance in terms of sample efficiency, estimator variance etc. Earlier attempts in combining nonlinear function approximators such as neural networks and RL were unsuccessful due to instabilities caused by 1) correlated training samples, 2) drastic change in policy with small change in function approximation, and 3) correlation between the training function and approximated function [10]. Success of DQN is attributed to addressing these issues with two key ingredients of the algorithm: **Experience Replay Memory** \mathbb{M} and **Target Network**, Q_{θ^*} . The replay memory stores the transitions of an MDP, specifically the tuple, (S_t, P_t, r_t, S_{t+1}) . The algorithm then samples, uniformly, a random minibatch of transitions from the memory. This removes correlation between the data and smoothens the data distribution change with iteration. The algorithm has another neural network, approximating the value function, Q_θ . The target network and randomly sampled mini-batch from the memory \mathbb{M} , form the training set for training the Q_θ , at every epoch. This random sampling provides *i.i.d* samples for performing stochastic gradient descent with loss:

$$L_Q^{\pi_\theta} = \frac{1}{n} \sum_{j=1}^n (Y_j - Q_\theta(S_j, A_j))^2 \quad (13)$$

where, $Y_i = r_i + \gamma \max_{a'} Q_{\theta^*}(S_i, a')$. The iterates $\{\theta_t\}$ are given by:

$$\theta_{t+1} \leftarrow \theta_t - \eta_1(t) \nabla_{\theta} L_Q^{\pi_\theta}, \quad (14)$$

where $\eta_1(t)$, the step size, satisfies:

$$\sum_{t=0}^{\infty} \eta_1(t) = \infty, \quad \sum_{t=0}^{\infty} \eta_1^2(t) < \infty, \quad \eta_1(t) \geq 0. \quad (15)$$

The weights of the target network Q^* are held constant for T_{target} epochs, thereby controlling any drastic change in policy and reducing correlation between Q and Q^* . This can be seen as a Risk Minimization problem in nonparametric-regression with regression function Q_{θ^*} and risk $L_Q^{\pi_{\theta^*}}$. Readers are referred to [16] for elaborate analysis of DQN. Theorem 4.4 in [16] provides a proof of convergence and the rate of convergence using non-parametric regression bounds, when sparse ReLU networks are used, under certain smoothness assumptions on the reward function and the dynamics.

B. Adaptive Constrained DQN (AC-DQN)

The DQN algorithm is meant for unconstrained optimization. Since our problem has an average power constraint of \bar{P} , we consider the instantaneous reward in (12), with a Lagrange multiplier β . The long term constraint depends on

the Lagrange multiplier and can be quite sensitive to it. Thus, we design our algorithm, AC-DQN, to learn the appropriate β . We will see later, that this will enable us to further modify our algorithm to track the changing statistics of the channel gains and arrival statistics. The AC-DQN algorithm is given in Algorithm 2. Here, we use multi-timescale SGD as in [9]. In this approach, in addition to the SGD on Q_θ , using minibatch, we use a stochastic gradient descent on the Lagrange constant, β as

$$\beta_{t+1} \leftarrow \beta_t + \eta_2(t) \nabla_\beta L_P^{\pi_\theta}, \quad (16)$$

where $\nabla_\beta L_P^{\pi_\theta} = C_P(S_t) - \bar{P}$. Since the expectation in (11) is not available to us, we take $C_P(S_t) = \sum_{i=t-T_W}^t P_i(S_i)/T_W$, where T_W is the finite horizon window. Additionally η_1 and η_2 are required to follow [9]:

$$\begin{aligned} \sum_{i=1}^{\infty} \eta_1(i) &= \sum_{i=1}^{\infty} \eta_2(i) = \infty, \\ \sum_{i=1}^{\infty} \eta_1^2(i) + \eta_2^2(i) &< \infty, \quad \frac{\eta_2(i)}{\eta_1(i)} \rightarrow 0. \end{aligned} \quad (17)$$

Algorithm 2: Adaptive Constrained DQN (AC-DQN) Algorithm

Input:

MDP($\mathcal{S}, \mathcal{A}, r, \mathbf{P}, \gamma$), r as in (12), Replay Memory: \mathbb{M} ,
 Minibatch size: n , Initialize $T, T_{target}, \theta, \theta^*$ of Q_θ and Q_{θ^*} ,
 Exploration Parameter: $\epsilon(t) \rightarrow 0$, Lagrange Constant: β , Value and Lagrange learning rates: $\eta_1(t), \eta_2(t)$ must satisfy (17), Initialize T_W

for $t = 1$ **to** T **do**

Observe state S_t , Apply action

$$A_t = \pi_t(S_t) = \arg \max_{a'} Q_\theta(S_t, a'), \quad \epsilon\text{-greedily}$$

Observe: r_t, S_{t+1}

Store: $(S_t, A_t, r_t, C_P(S_t), S_{t+1})$ in \mathbb{M}

Sample: Minibatch n from \mathbb{M}

for $i = 1$ **to** n **do**

$$| \quad Y_i = r_i + \gamma \max_{a'} Q_{\theta^*}(S_{i+1}, a')$$

end

/*Perform two time-scale stochastic gradient descent as follows:*/

$$\theta \leftarrow \theta - \eta_1 \nabla_\theta L_Q^{\pi_\theta}$$

$$\beta \leftarrow \beta + \eta_2 \nabla_\beta L_P^{\pi_\theta}$$

at every $t = mT_{target}, m \in \mathbb{N}^+$: update $\theta^* \leftarrow \theta$

end

$$\pi^* \leftarrow \pi_T, \theta^* \leftarrow \theta$$

Output: Q_{θ^*} : Optimal Q -Function, π : Optimal Policy

Tracking with AC-DQN: Tracking of system statistics is essential, to achieve optimal power control in a non-stationary system. In multi-time scale stochastic gradient descent, such as AC-DQN, step sizes $\eta_1(t)$ and $\eta_2(t)$ can be fixed to enable tracking. If $\eta_2 \ll \eta_1$, then the Lagrange multiplier changes much more slowly than the Q -function. Then the two timescale theory (see, e.g., [9]), will allow the Lagrange multiplier to adapt slowly to the changing system statistics but at the same time provide average power control. The solution will

reach in a neighbourhood of the optimal point. Although the convergence of this modified algorithm is not proved yet (even for the unconstrained DQN, convergence has been proved only recently in [16]), our simulations will show that the resulting algorithm tracks the optimal solution in the time varying scenario.

The time varying scenario in our setup results due to change in the request arrival statistics from the users and changing channel gain statistics due to motion of the users.

VI. INTEGRATED DSGD AND AC-DQN (IDA)

We are now familiar with how multi-time scale stochastic gradient descent can be used for optimization of a stochastic system with multiple objectives. We extend this idea to learn the optimal queueing strategy while learning the optimal power control policy and simultaneously satisfying the average power constraint. Towards this we add DSGD as a third timescale to AC-DQN. Though DSGD internally has two stochastic gradient descent steps, we consider it as a combined third step of IDA for conceptual clarity. We present our Integrated DSGD and AC-DQN (IDA) in Algorithm 3. There are four learning rates involved in the algorithm. The four learning rates are supposed to satisfy the following criteria for convergence of the algorithm [9]:

$$\begin{aligned} \sum_{i=1}^{\infty} \eta_j(i) &= \infty, \quad j = 1, 2, 3, 4, \\ \sum_{i=1}^{\infty} \sum_{j=1}^4 \eta_j^2(i) &< \infty, \quad \frac{\eta_{j+1}(i)}{\eta_j(i)} \rightarrow 0, \quad j = 1, 2, 3. \end{aligned} \quad (18)$$

Though this criterion is required for convergence, we have seen that constant step sizes are helpful in tracking. So we will see our simulations with $\eta_1 > \eta_2 > \eta_3/T_{approx} > \eta_4/T_{approx}$.

We note the following:

- This is a generalized algorithm that can be used in systems where multiple objectives are to be met simultaneously such as in cross-layer designs in wireless networks.
- In applying multi-time scale stochastic optimization, it is necessary to identify which parameters are to be learnt in a faster timescale and which in slower. In IDA we learn the queueing strategy in a slower time scale and the power control policy on a faster timescale. To have a meaningful update of Q -function network θ , it is necessary that the underlying MDP doesn't change drastically. This is ensured by updating the θ^\dagger and queueing strategy \bar{p} at a much slower rate as compared to the θ and θ^* updates.
- In practical systems, where the systems statistics are usually non-stationary, the learning rate selection ($\eta_i, i = 1, 2, 3, 4$ selection) is the most important engineering decision. This controls the trade-off between speed and stability of the algorithm. Learning rates must be carefully selected to ensure that the parameter updates are neither too slow to track the changing system statistics nor too fast for stability of the learning algorithm.

Algorithm 3: Integrated DSGD and AC-DQN Algorithm (IDA)

Input:

DQN Input: MDP- $(\mathbb{S}, \mathbb{A}, r, \mathbf{P}, \gamma)$, r as in (12), \mathbb{M} , n , T , T_{target} , θ, θ^* of Q_θ, Q_{θ^*} , $\epsilon(t) \rightarrow 0$, $\beta, \eta_1(t) \rightarrow 0$, $\eta_2(t) \rightarrow 0$ and T_W are same as in Algorithm 2,

DSGD Inputs: Replay Memory: \mathbb{M}_D , Minibatch size: n_D , Training Time: S_{train} , Approximation Window: T_{approx} , Initialize weights θ^\dagger of f_{θ^\dagger} , Exploration Parameter: $\epsilon_D(s) \rightarrow 0$, Learning rates: $\eta_i, i = 1, 2, 3, 4$ satisfy, (18), System timeline: t , DSGD timeline: s , $s \leftarrow 0$, $\bar{p} \leftarrow \mathcal{P}(Unif([0, 1]^3))$

for $t = 1$ **to** T **do**

Observe S_t , Take action A_t and store

$(S_t, A_t, r_t, C_P(S_t), S_{t+1})$ in \mathbb{M}

Sample: Minibatch n from \mathbb{M} as in Algorithm 2

/*Perform two time-scale stochastic gradient descent as follows:*/

$\theta \leftarrow \theta - \eta_1 \nabla_\theta L_Q^{\pi_\theta}$,

$\beta \leftarrow \beta + \eta_2 \nabla_\beta L_P^{\pi_\theta}$

at every $t = mT_{target}, m \in \mathbb{N}^+$: update $\theta^* \leftarrow \theta$

$\bar{D} \leftarrow \text{append}(\text{sojourntime } d_i^s)$ in current service

if $t = mT_{approx}, m \in \mathbb{N}^+$ **then**

if $(s < S_{train})$ **then**

| $\bar{p} \leftarrow \mathcal{P}(Unif([0, 1]^3))$

else

| **Sample:** Minibatch n_D from \mathbb{M}_D

| /*Perform DNN θ^\dagger update and \bar{p} parameter update as follows:*/

| $\theta^\dagger \leftarrow \theta^\dagger - \eta_3 \nabla_{\theta^\dagger} L_{f_{\theta^\dagger}}$,

| $\bar{p} \leftarrow \mathcal{P}(\bar{p} - \eta_4 \nabla_{\bar{p}} f_{\theta^\dagger}(\bar{p}) + Unif([0, \epsilon_D(s)]^3))$

end

obtain \hat{f} , as in (1)

clear \bar{D}

store (\bar{p}, \hat{f}) in \mathbb{M}_D

$s \leftarrow s + 1$

end

$\bar{p}^* \leftarrow \bar{p}$, $\pi^* \leftarrow \pi_T$, $\theta^* \leftarrow \theta$

Output: \bar{p}^* : Optimal Queuing Strategy, Q_{θ^*} : Optimal Q-Function, π : Optimal Policy

We now present simulation results of all the algorithms presented in this paper.

VII. SIMULATION RESULTS AND DISCUSSION

In this section, we first present simulation results for our DSGD algorithm. We run the multicast system with constant transmit power. We compare the performance of our DSGD queuing algorithm against each queuing strategy proposed in [8]. Next, we demonstrate the Deep Learning methods for power control proposed in this paper. We compare the performances of AC-DQN and MADS Power control policies. Though MADS provides optimal solutions for small system sizes, it is not scalable. We show that the Deep Learning algorithm, AC-DQN, indeed achieves the global optimum obtained by MADS algorithm, while being scalable with the

system size (number of users). We further demonstrate that AC-DQN algorithm tracks the changing system dynamics and obtains the optimal policy, adaptively. Finally, we present our integrated algorithm for optimal queuing and power control, the IDA algorithm. We show, numerically, that the algorithm achieves the optimal point obtained by both DSGD and AC-DQN. Our multicast system is implemented in Python and we use Keras libraries in Python for implementation of our algorithms¹.

A. Simulation parameters

We consider three systems with varying system configurations as follows:

1) **Small User Case:** Number of users, $L = 4$, Catalog Size $M = 100$, File Size $F = 10MB$, Transmission rate $C = 10MB/s$, Bandwidth $B = 10MHz$, Channel Gains \sim Uniform([0.1 0.2 0.3]) for two users with bad channel statistics and \sim Uniform([0.7 0.8 0.9]) for two users with good channel statistics, File Popularity: Uniform, (Zipf exponent = 0), Average Power Constraint $\bar{P} = 7$, Simulation time = 10^5 multicast transmissions.

2) **Moderate User Case:** System Parameters: Power Transmit Levels = 20 (1 to 50), $L = 10$, $M = 100$, $F = 10MB$, $C = 10MB/s$, Channel Gains: Exponentially distributed ($\sim \exp(0.1)$ for bad channel, $\sim \exp(1.0)$ for good channel), $R = 10MB/s$, $B = 10MHz$, $\bar{P} = 7$, File Popularity: Zipf distribution with Zipf exponent = 1. Simulation time: 10^5 multicast transmissions. In both the cases, we set the noise power as $N_g = 1$.

3) **Large User Case:** System Parameters: Same as VII-A2 except, $L = 20$.

4) **Hyperparameters:** For DSGD, we consider a fully connected neural network with two hidden layers. First layer has 32 nodes and second layer has 16 nodes. All layers have ReLU activation function. $\mathbb{M}_D = 1000$, Minibatch size: $n_D = 50$, $T_{train} = 100$: Training Time, $S_{approx} = 100$: Approximation Window, Initialize weights θ of f_θ , $\epsilon(t) \rightarrow 0$, $\eta_1(t) = .01/(1 + .00001t)$, $\eta_2(t) = .001/(1 + .00001t \log(\log(t)))$.

In AC-DQN, we consider fully connected neural networks with two hidden layers for all the function approximations considered in the algorithms. Input layer nodes are assumed to be $2L$ and the output layer nodes is equal to 20, the number of transmit power levels. Each output represents the Q value for a particular action. The action space is restricted to be finite, as DQN converges only with finite action spaces. We use two hidden layers for the neural network, with 128 and 64 nodes, and ReLU activation function is chosen, respectively. The other parameters are as follows: Replay memory size $|\mathbb{M}| = 30000$, $\gamma = 0.9$, $\epsilon_0 = 1.0$, $\epsilon_{decay} = 0.98$, $\epsilon_t = \epsilon_0(0.98)^t$, $\eta_1 = 0.001$, $\eta_1^{decay} = 0.00001$, $\eta_2 = .0001$, $\eta_2^{decay} = 0.00001$, Mini-batch Size (n) = 64, $T_{target} = 100$, and $T_W = 200$.

Finally, in IDA algorithm we combine the parameters of both DSGD and AC-DQN. Step sizes are however held constant with value of each step size at $t = 0$.

¹The system and algorithm codes are available in https://github.com/rkragh88/SchedulingPC_IDA

B. Optimal Queueing using DSGD

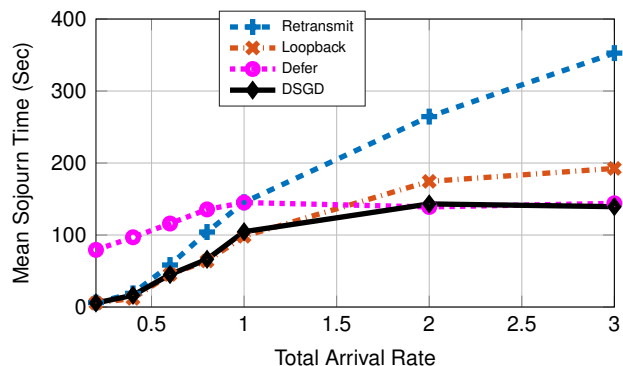
We consider the moderate user system in section VII-A2 for demonstrating the performance of DSGD. We assume the widely accepted IRM traffic model, with unity zipf popularity for the 100 different file requests arriving at 10 users. The server is endowed, in different simulation runs, with different queueing strategies. We compare our DSGD based queueing strategy at server with the individual queueing strategies, mentioned in section II. The server transmits the files with constant transmit power $\bar{P} = 7$. We model the wireless fading to follow Rayleigh distribution. This introduces the errors in file transmissions.

We see in Figure 2a that different queueing strategies are optimal at different rates for a constant transmit power $\bar{P} = 7$ under fading. This is the typical case in practical systems. Depending on the request load the system might need to adapt the queueing and service strategy. DSGD does precisely this. We can see in Figure 2b that the algorithm converges to the optimal mean sojourn time for the given power policy. We use constant transmit power policy. Epochs 0 to 10^4 are the initial training phase and the algorithm starts learning thereafter and eventually converges. The policy chosen by the algorithm for arrival rates 0.6 and 3.0 are given in Figures 3a and 3b, respectively. We see that for rate 3.0, the algorithm converges to the defer strategy since it has the lowest mean sojourn time for this rate (Fig 2a). For rate 0.6 however we see that DSGD gives a mixed policy with positive probabilities to retransmit and loopback and zero probability to defer. This is because both retransmit and loopback have the same mean delay performance and the defer strategy performs poorly. This is the case where more than one optimal solution may be available and the algorithm may converge to one or oscillate between different optimal points, as neural network training progresses. The simulations show that the DSGD algorithm chooses the best among the three queueing policies or an equivalent mixed policy for different system statistics (arrival rates). This shows that the DSGD adapts to the system statistics which is very important in a practical system. We will see in subsequent sections that the adaptability of DSGD is very useful in cross-layer system optimization of the Multicast network.

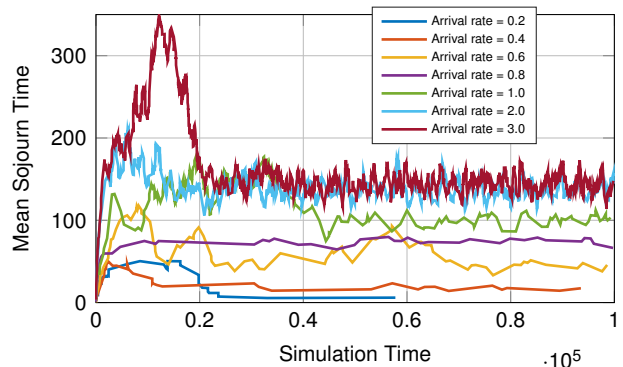
C. Optimal power control (AC-DQN vs MADS):

We use the system setting of small user case, specified in VII-A1, since running MADS for higher number of users is computationally prohibitive. We use uniform popularity profile for the file requests. We also use uniform distribution for fading. This is just for the convenience of calculations of state probabilities, $\{q_k\}$, in MADS as done in [8]. We compare the performance of AC-DQN and MADS for this system. We demonstrate our algorithm with more realistic distribution in the next section.

We use the Loopback queueing strategy for demonstrating AC-DQN. We will see in subsequent sections that AC-DQN works even for other queueing strategies. We split the users in two equal sized groups, one group has good channel statistics and the other bad channel statistics, to show the advantage of power control. We compare both power control policies



(a) DSGD Mean Sojourn Times vs Arrival Rate.



(b) DSGD Convergence of Mean Sojourn Time.

Fig. 2: DSGD Performance in parametrized multicast system with constant power policy, $L = 10$, $\bar{P} = 7$, Zipf Popularity (Zipf exponent =1), Rayleigh fading with mean, 0.1 and 1.0 for bad and good users respectively.

with a constant power control policy, where the transmit power P_t is fixed to $P_t = \bar{P}$, to indicate the gain due to power control. Figure 4a shows a comparison of mean sojourn times of Constant Power Policy, $P_t = \bar{P}$, MADS and AC-DQN. Further, Figure 4b shows convergence of average power to \bar{P} for AC-DQN. We see from Figure 4b that AC-DQN achieves the same mean sojourn time as that by MADS, while maintaining the average power constraint. Further we demonstrate power control by AC-DQN for a scaled up system with 20 users.

D. AC-DQN performance in a Scaled Network:

To show the scalability of AC-DQN. We simulate the relatively complex system mentioned in large user case, section VII-A3. We use Zipf Popularity, Rayleigh fading (refer Section VII-A3) to analyse AC-DQN on a more realistic system. We use Loopback queueing strategy at the server and run the simulation for the average power constraint $\bar{P} = 7$. We see in Figure 5a that the AC-DQN gives, drastic improvement (around 50 percent) over constant power case. AC-DQN achieves this while maintaining the average power, by learning the Lagrange constant as seen in Figure 5c. Figure 5b shows the convergence of average power of AC-DQN to the average power constraint, \bar{P} , for arrival rate of 1.0 requests per sec in the same simulation run.

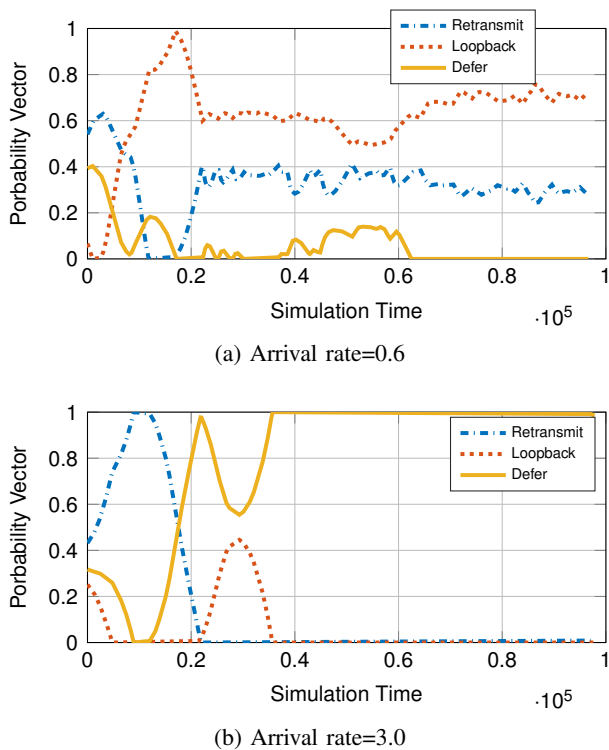


Fig. 3: Probability convergence for $L = 10$, $\bar{P} = 7$, Zipf Popularity (Zipf exponent =1), Rayleigh fading with mean, 0.1 and 1.0 for bad and good users respectively.

E. AC-DQN Tracking Simulations:

In this section, we show via simulations, the tracking capabilities of AC-DQN for the large user case (section VII-A3). We demonstrate the importance of constant step sizes for η_1 and η_2 , and the inability of decaying step sizes to track the changing system statistics. We consider a system where the arrival rates change over a period of 48 hours. We fix $\lambda = 1.0$ for first 24 hours. To make the learning harder for our algorithm, we change the rates abruptly, every six hours for next 24 hours as $\lambda = 0.6, 0.5, 0.4, 0.8$. This change in time period is just to illustrate the tracking ability in a more emphatic manner. This also captures the real world scenario where the request traffic to the base station varies with time of the day. We fix $\bar{P} = 5$. We calculate the mean sojourn time and average power using a moving average window of size 1000 samples. We run the AC-DQN algorithm for this system with: 1) decaying η_1 and η_2 satisfying (17) and 2) constant step sizes, $\eta_1 = 0.001$ and $\eta_2 = 0.00003$. Rest of the parameters remain same as in the large user case. We see in Figure 6a that the AC-DQN with constant step-size almost always outperforms the decaying step size. Specifically, after the first 24 hours the delay reduction is nearly 50 percent for constant step-size. The reason for this is evident from Figures 6b and 6c. We see in Figure 6c that the AC-DQN with constant step-size learns the Lagrange constant through out the simulation time, whereas, the AC-DQN decaying step size is unable to learn the Lagrange constant after the first 24 hours. As can be seen in Figure 6b, this affects the average power achieved by the AC-DQN with decaying step size. While constant step

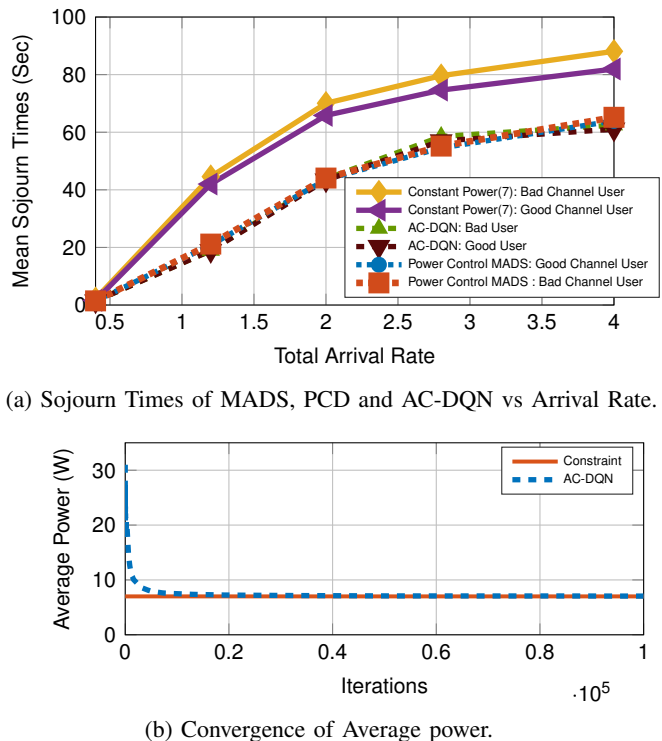
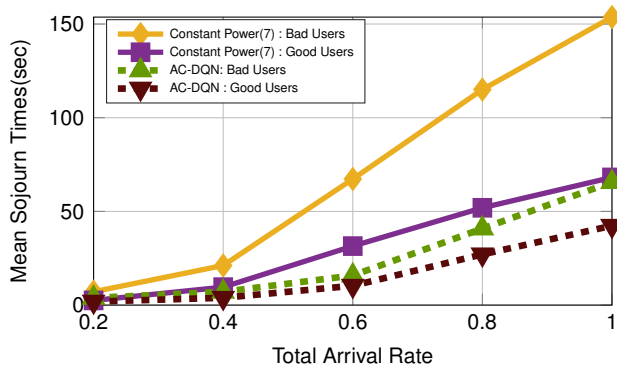


Fig. 4: AC-DQN Performance in 1-LB system with $L = 4$, $\bar{P} = 7$, Uniform Popularity, Uniform fading.

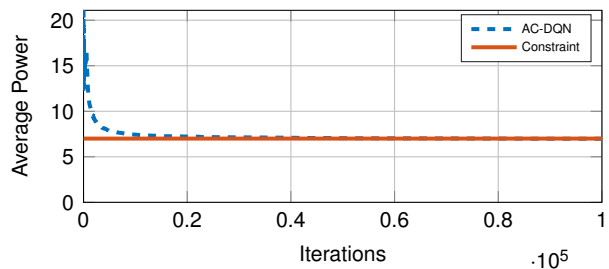
size maintains the average power constraint of $\bar{P} = 5$, the average power achieved by the decaying step-size AC-DQN drops to 4. Hence, the decaying step-size AC-DQN suffers suboptimal utilization of available power. Thus in practical systems, only constant step-size AC-DQN will be capable of adapting to the changing system statistics. The effect of fixing the learning rates is seen in the small oscillations of average power around $\bar{P} = 5$ in Figure 6b. This is the oscillation in a small neighborhood around the optimal average power. Smaller the step size, lesser the oscillations.

F. Integrated Optimal Queueing and Power Control using IDA

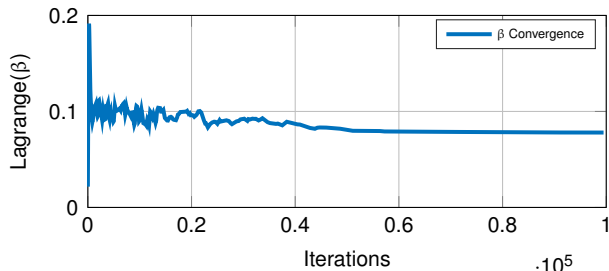
We have already seen the performance of power control for 1LB (Loopback case) for large user system. In this section we compare the performances of AC-DQN for different queueing strategies versus the IDA performance for the moderate user case (Section VII-A2). We use Zipf popularity and Rayleigh fading for system simulation. First, in Figure 7a, we make an observation that AC-DQN drastically improves the mean delay performance for all the strategies as compared to the constant power policy in Figure 2a. We see that our IDA algorithm is able to choose better strategy than the baselines in terms of mean sojourn time. The convergence of mean sojourn time for rates 0.2 to 3.0 is shown in Figure 7b. The more important capability of this algorithm is that it converges to a better mean sojourn time while maintaining the average power constraint. Figure 7c shows convergence of the average power to $\bar{P} = 7$ for all the rates. This is achieved by simultaneously controlling the Lagrange variable as seen in Figure 7d. A few interesting



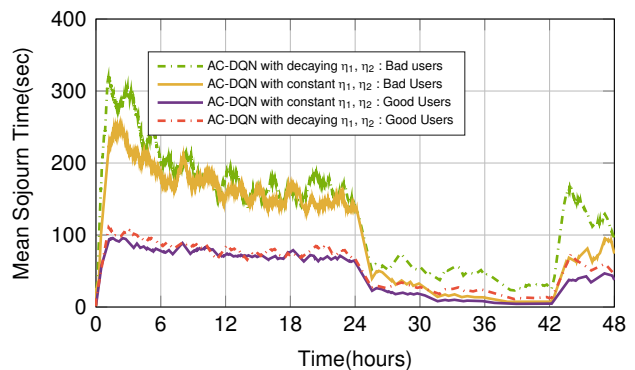
(a) Constant Power and AC-DQN vs Arrival Rate



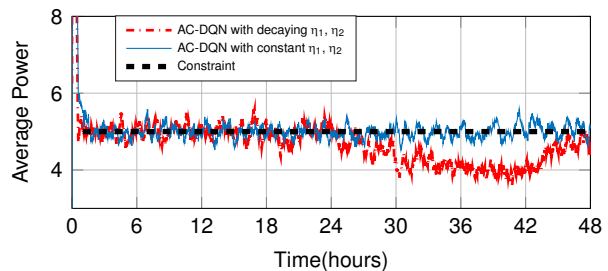
(b) Average Power Convergence.



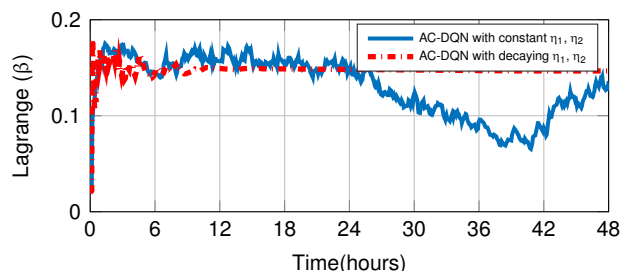
(c) Lagrange Convergence.



(a) Mean Sojourn Time tracking



(b) Average Power



(c) Lagrange

Fig. 5: AC-DQN Performance in 1-LB system with $L = 20$, $\bar{P} = 7$, Zipf(1) Popularity, Rayleigh fading.

plots showing convergence of probabilities for rates 0.8, 2.0 and 3.0 are shown in Figures 8a, 8b and 8c respectively.

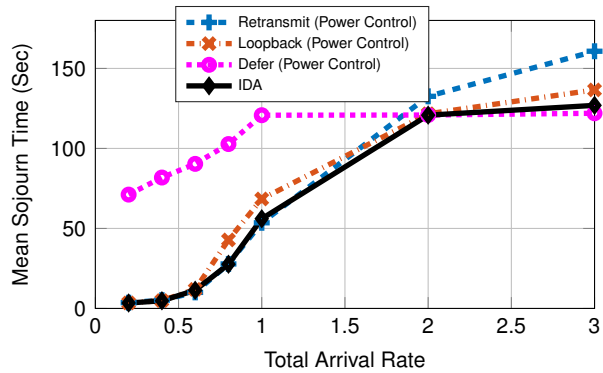
We see, in 8a, for arrival rate 0.8, that the probability converges to a mixed policy with 0.8 probability assigned to retransmit and 0.2 assigned to loopback, though we see in Figure 7a that retransmit individually has the same optimal mean sojourn time as achieved by IDA. This is attributed to more flexibility available with the algorithm. If the DeepRL in IDA finds an optimal power control policy along with this mixed policy that achieves the optimal mean delay, it may converge to that policy. In other words this flexibility gives additional optimal points for the algorithm, to choose from. Infact, we see that in Figure 8a that the algorithm first goes to retransmit and eventually converges to this mixed policy, while maintaining average power and optimal delay throughout. For rate 0.2 both defer and loopback have same AC-DQN performance Figure 7a. Hence, the solution oscillates between them Figure 8b, while maintaining the average power and

Fig. 6: AC-DQN Tracking Performance in 1-LB system with with decaying vs constant step-sizes $L = 20$, $\bar{P} = 7$, Zipf(1) Popularity, Rayleigh fading.

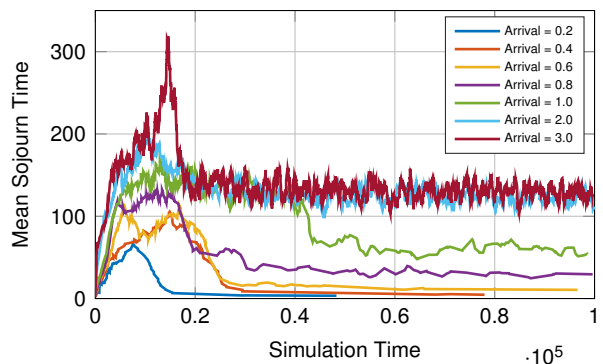
optimal delay. For arrival rate 3.0, Figure 8c, however the algorithm unambiguously chooses defer as the policy since it has the lowest mean sojourn time among the baselines, Fig 7a. The simulations show that IDA is able to achieve adaptive cross-layer optimization of queueing and power control simultaneously, for different system statistics (arrival rates).

G. Discussion:

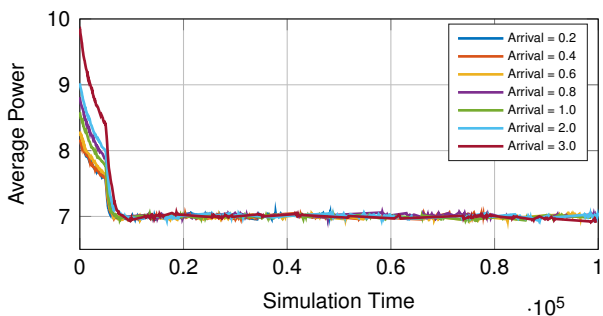
We see from the simulations that the novel Deep Learning techniques such as DSGD and AC-DQN can achieve optimal performance while providing scalability with system size. We have demonstrated how DNNs can be used for noise reduction in gradient estimates in a stochastic gradient descent algorithm, as done in DSGD. Our two-timescale approach, AC-DQN, extends DeepRL algorithms like DQN to systems with constrained control. Though we have demonstrated this on a system with a single constraint, it can be extended



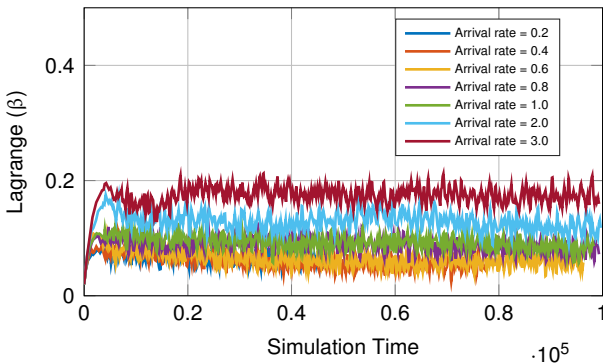
(a) IDA Mean Sojourn Times vs Arrival Rate



(b) IDA Convergence of Mean Sojourn Time.

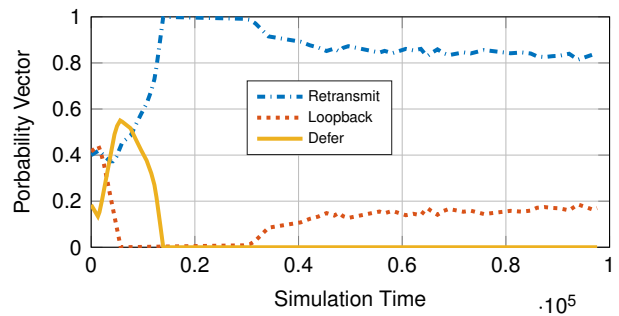


(c) IDA Average Power Convergence

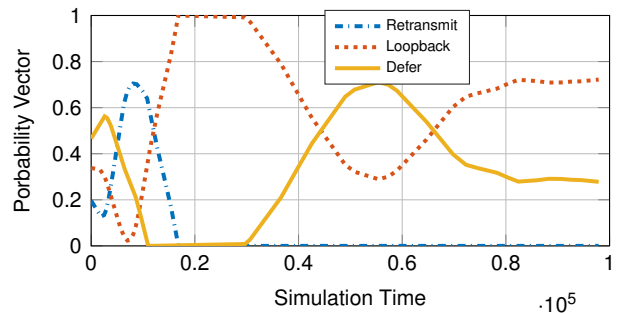


(d) IDA Lagrange Convergence

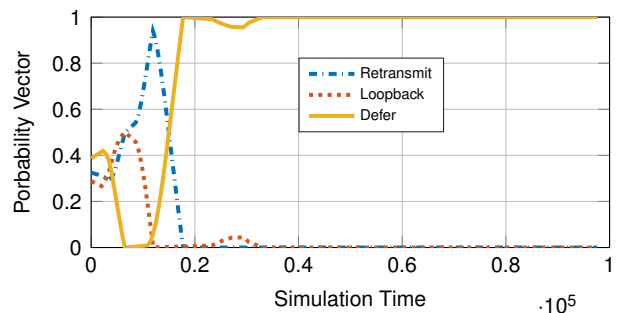
Fig. 7: IDA Performance in parametrized multicast system with $L = 10$, $\bar{P} = 7$, Zipf Popularity (Zipf exponent =1), Rayleigh fading with mean, 0.1 and 1.0 for bad and good users respectively.



(a) Arrival rate=0.8



(b) Arrival rate=2.0



(c) Arrival rate=3.0

Fig. 8: IDA convergence of queuing strategies for different arrival rates. $L = 10$, $\bar{P} = 7$, Zipf Popularity (Zipf exponent =1), Rayleigh fading with mean, 0.1 and 1.0 for bad and good users respectively.

to systems with multiple constraints. In such systems each constraint is associated with a Lagrange multiplier. Each Lagrange multiplier adds an additional SGD step to the AC-DQN algorithm. For a stationary system, it is enough that the step-sizes satisfy multi-timescale criterion similar to (17), see [9]. However, if AC-DQN is used in systems with changing system statistics the step sizes shall be kept constant. The step sizes shall be fixed as per the tolerance requirement for a given constraint (e.g., in our system the tolerance could be $\bar{P} \pm \Delta P$, where, ΔP is the allowed deviation from the constraint \bar{P}). Lesser the tolerance, lesser the step-size. However, fixing the step-sizes too small may make the algorithm too slow to track the changes in system statistics. Hence, choosing the step sizes is a trade-off between the tolerance of the constraint and the required algorithmic agility to track the system changes. We have shown that this Multi-

timescale approach in AC-DQN can very well be extended to systems with multiple objectives as demonstrated by our IDA algorithm. We have also demonstrated how IDA achieves the optimal queuing strategy among the baselines while obtaining the power control for such complex multicast systems. It is shown that Deep Neural Networks when appropriately used can provide scalable control for large wireless networks. Infact it can simultaneously achieve several cross-layer objectives even in large wireless networks for providing optimal QoS.

VIII. CONCLUSION

This paper considered a multicast downlink in single hop wireless network. Fading of different links to users causes significant reduction in the performance of the system. Appropriate change in the queueing policies and power control can mitigate most of the losses. However, simultaneously obtaining adaptive queueing and power control for large systems is computationally very hard. We first develop a novel DNN assisted stochastic gradient descent algorithm to achieve optimality of the system to provide lower mean sojourn time in a parametrized multicast system. Next we show that using Deep Reinforcement Learning, we can obtain optimal power control, online, even when the system statistics are unknown. We use a recently developed version of Q learning, Deep Q Network to learn the Q-function of the system via function approximation. Furthermore, we modify the algorithm to satisfy our constraints and also to make the optimal policy track the time varying system statistics. Finally, we propose a novel deep multi-time scale algorithm which achieves the cross-layer optimization of queueing and power control, simultaneously.

One interesting extension of this work would be developing an algorithm that could potentially provide better state-action dependent queueing strategy. Another future work could possibly include, the caches at the user nodes and learning the optimal caching policy along with the power control using DeepRL. Future works may also consider applying IDA to multiple-base-station scenarios for interference mitigation.

REFERENCES

- [1] Cisco, "Cisco visual networking index: global mobile data traffic forecast update 2016-2021 white paper," 2016.
- [2] M. Cha, H. Kwak, P. Rodriguez, Y.-Y. Ahn, and S. Moon, "I tube, you tube, everybody tubes: Analyzing the world's largest user generated content video system," in *Proc. 7th ACM SIGCOMM Conf. on Internet Measure.*, 2007, pp. 1–14.
- [3] N. Moghadam and H. Li, "Improving queue stability in wireless multicast with network coding," *IEEE Inter. Conf. on Commun. (ICC)*, pp. 3382–3387, 2015.
- [4] R. Cogill and B. Shrader, "Queue length analysis for multicast: Limits of performance and achievable queue length with random linear coding," in *47th Allerton Conf on Commun., Control, and Comp.*, 2009, pp. 462–468.
- [5] M. A. Maddah-Ali and U. Niesen, "Fundamental limits of caching," *IEEE Trans. Inf. Theory*, vol. 60, pp. 2856–2867, 2014.
- [6] F. Rezaei and B. H. Khalaj, "Stability, rate, and delay analysis of single bottleneck caching networks," *IEEE Trans. Commun.*, vol. 64, no. 1, pp. 300–313, 2016.
- [7] M. Panju, R. Raghu, V. Sharma, and R. Ramachandran, "Queueing theoretic models for multicast and coded-caching in downlink wireless systems," *arXiv:1804.10590*, 2018.
- [8] M. Panju, R. Raghu, V. Agarwal, V. Sharma, and R. Ramachandran, "Queueing theoretic models for multicasting under fading," *IEEE Wireless Communications and Networking Conference (WCNC), Marrakech, Morocco*, 2019.
- [9] V. Borkar, *Stochastic Approximation: A Dynamical Systems Viewpoint*. Cambridge University Press, 2008.
- [10] Y. Li, "Deep reinforcement learning," *CoRR*, 2018. [Online]. Available: <http://arxiv.org/abs/1810.06339>
- [11] V. Mnih *et al.*, "Human-level control through deep reinforcement learning," *Nature*, vol. 518, Feb 2015.
- [12] J. Schulman *et al.*, "Trust region policy optimization," in *Inter. Conf. Machine Learning*, 2015, pp. 1889–1897.
- [13] —, "Proximal policy optimization algorithms," *arXiv: 1707.06347*, 2017.
- [14] V. Mnih *et al.*, "Playing atari with deep reinforcement learning," *NIPS Deep Learning Workshop*, 2013.
- [15] D. Silver *et al.*, "A general reinforcement learning algorithm that masters chess, shogi, and go through self-play," *Science*, vol. 362, no. 6419, pp. 1140–1144, 2018.
- [16] Z. Yang, Y. Xie, and Z. Wang, "A theoretical analysis of deep q-learning," *arXiv: 1901.00137*, 2019.
- [17] H. Van Hasselt, A. Guez, and D. Silver, "Deep reinforcement learning with double q-learning," in *Thirtieth AAAI Conference on Artificial Intelligence*, 2016.
- [18] N. Moghadam, H. Li, H. Zeng, and L. Liu, "Lyapunov scheduling and optimization in network coded wireless multicast network," *IEEE Transactions on Vehicular Technology*, vol. 67, no. 6, pp. 5135–5145, 2018.
- [19] N. Moghadam, G. Zhang, and H. Li, "Simplified optimal scheduling (sos) for network coded wireless multicast," in *2018 IEEE 88th Vehicular Technology Conference (VTC-Fall)*, 2018, pp. 1–5.
- [20] Y. Zhou *et al.*, "Multicast scheduling for delay-energy trade-off under bursty request arrivals in cellular networks," *IET Comm.*, vol. 13, pp. 1696–1701(5), 2019.
- [21] N. Jindal and A. Goldsmith, "Capacity and optimal power allocation for fading broadcast channels with minimum rates," *IEEE Transactions on Information Theory*, vol. 49, no. 11, pp. 2895–2909, Nov 2003.
- [22] K. Wang, C. F. Chiasserini, R. R. Rao, and J. G. Proakis, "A distributed joint scheduling and power control algorithm for multicasting in wireless ad hoc networks," in *IEEE Intern. Conf. on Comm.*, vol. 1, 2003, pp. 725–731.
- [23] H. Ye, G. Y. Li, and B. F. Juang, "Deep reinforcement learning based resource allocation for v2v communications," *IEEE Transactions on Vehicular Technology*, vol. 68, no. 4, pp. 3163–3173, April 2019.
- [24] Y. S. Nasir and D. Guo, "Multi-agent deep reinforcement learning for dynamic power allocation in wireless networks," *arXiv*, 2018. [Online]. Available: <http://arxiv.org/abs/1808.00490v3>
- [25] Z. Zhang *et al.*, "Double coded caching in ultra dense networks: Caching and multicast scheduling via deep reinforcement learning," *IEEE Trans. Comm.*, vol. 68, no. 2, pp. 1071–1086, 2020.
- [26] Q. Mao, F. Hu, and Q. Hao, "Deep learning for intelligent wireless networks: A comprehensive survey," *IEEE Communications Surveys Tutorials*, vol. 20, no. 4, pp. 2595–2621, 2018.
- [27] E. Altman, *Constrained Markov Decision Processes*. CRC Press, 1999.
- [28] J. Achiam *et al.*, "Constrained policy optimization," in *Proc. Intern. Conf. on Machine Learning*, 2017, pp. 22–31.
- [29] C. Tessler, D. J. Mankowitz, and S. Mannor, "Reward constrained policy optimization," *arXiv: 1805.11074*, 2018.
- [30] M. Yu *et al.*, "Convergent policy optimization for safe reinforcement learning," in *Advances in NIPS*, 2019, pp. 3127–3139.
- [31] P. Sadeghi, R. A. Kennedy, P. B. Rapajic, and R. Shams, "Finite-state markov modeling of fading channels - a survey of principles and applications," *IEEE Signal Processing Magazine*, vol. 25, no. 5, pp. 57–80, September 2008.
- [32] S. Bhatnagar, H. Prasad, and L. Prashanth, *Stochastic Recursive Algorithms for Optimization: Simultaneous Perturbation Methods*. Springer London, 2013.
- [33] B. Hanin, "Universal function approximation by deep neural nets with bounded width and relu activations," *Open Access Journals MDPI, Mathematics*, vol. 7, no. 10, 2019. [Online]. Available: <https://www.mdpi.com/2227-7390/7/10/992>
- [34] D. Rolnick *et al.*, "Deep learning is robust to massive label noise," *arXiv: 1705.10694*, 2017.
- [35] T. Nguyen-Thien and T. Tran-Cong, "Approximation of functions and their derivatives: A neural network implementation with applications," *Applied Mathematical Modelling*, vol. 23, pp. 687 – 704, 1999.
- [36] L.-J. Lin, "Self-improving reactive agents based on reinforcement learning, planning and teaching," *Machine Learning*, vol. 8, no. 3, pp. 293–321, May 1992. [Online]. Available: <https://doi.org/10.1007/BF00992699>

- [37] A. Katharopoulos and F. Fleuret, "Not all samples are created equal: Deep learning with importance sampling," *CoRR*, vol. abs/1803.00942, 2018. [Online]. Available: <http://arxiv.org/abs/1803.00942>
- [38] D. P. Kingma and J. Ba, "Adam: A method for stochastic optimization," *arXiv: 1412.6980*, 2014.
- [39] J. Proakis and M. Salehi, *Digital Communications*, 5th ed. McGraw-Hill, 2008.
- [40] C. Audet and J. E. Dennis Jr, "Mesh adaptive direct search algorithms for constrained optimization," *SIAM Journal on optimization*, vol. 17, no. 1, pp. 188–217, 2006.
- [41] M. L. Puterman, *Markov Decision Processes: Discrete Stochastic Dynamic Programming*, 1st ed. J. Wiley & Sons, Inc., 1994.
- [42] T. P. Lillicrap *et al.*, "Continuous control with deep reinforcement learning," *arXiv: 1509.02971v5*, 2016.